Journal of Magnetic Resonance 214 (2012) 22–28

Contents lists available at SciVerse ScienceDirect

Journal of Magnetic Resonance

journal homepage: www.elsevier.com/locate/jmr

Dynamic changes in oxygenation of intracranial tumor and contralateral brain during tumor growth and carbogen breathing: A multisite EPR oximetry with implantable resonators

Huagang Hou [a,*], Ruhong Dong [a], Hongbin Li [a], Benjamin Williams [a], Jean P. Lariviere [a], S.K. Hekmatyar [b], Risto A. Kauppinen [b], Nadeem Khan [a], Harold Swartz [a]

[a] EPR Center for the Study of Viable Systems, Department of Radiology, Dartmouth Medical School, Hanover, NH 03755, United States
[b] NMR Research Center, Department of Radiology, Dartmouth Medical School, Hanover, NH 03755, United States

ARTICLE INFO

Article history:
Received 14 July 2011
Revised 19 September 2011
Available online 1 October 2011

Keywords:
Carbogen
EPR oximetry
F98 glioma
Implantable resonator
Intracranial tumor
pO_2

ABSTRACT

Introduction: Several techniques currently exist for measuring tissue oxygen; however technical difficulties have limited their usefulness and general application. We report a recently developed electron paramagnetic resonance (EPR) oximetry approach with multiple probe implantable resonators (IRs) that allow repeated measurements of oxygen in tissue at depths of greater than 10 mm.
Methods: The EPR signal to noise (*S*/*N*) ratio of two probe IRs was compared with that of LiPc deposits. The feasibility of intracranial tissue pO_2 measurements by EPR oximetry using IRs was tested in normal rats and rats bearing intracerebral F98 tumors. The dynamic changes in the tissue pO_2 were assessed during repeated hyperoxia with carbogen breathing.
Results: A 6–10 times increase in the *S*/*N* ratio was observed with IRs as compared to LiPc deposits. The mean brain pO_2 of normal rats was stable and increased significantly during carbogen inhalation in experiments repeated for 3 months. The pO_2 of F98 glioma declined gradually, while the pO_2 of contralateral brain essentially remained the same. Although a significant increase in the glioma pO_2 was observed during carbogen inhalation, this effect declined in experiments repeated over days.
Conclusion: EPR oximetry with IRs provides a significant increase in *S*/*N* ratio. The ability to repeatedly assess orthotopic glioma pO_2 is likely to play a vital role in understanding the dynamics of tissue pO_2 during tumor growth and therapies designed to modulate tumor hypoxia. This information could then be used to optimize chemoradiation by scheduling treatments at times of increased glioma oxygenation.
Published by Elsevier Inc.

1. Introduction

The oxygen level in solid tumors is an extremely important parameter that compromises the outcome of chemoradiation [1–3]. Tumor hypoxia ($pO_2 < 10 - 15$ mm Hg) also leads to the development of aggressive phenotypes and tumor metastases [1–3]. Because the oxygen levels in tumors change as tumors grow, and are also dynamically altered by treatment, it is very desirable to be able to monitor the oxygen level before, during, and after therapeutic interventions.

Given the significant role of hypoxia in therapeutic resistance, several approaches have been tested to counteract tumor hypoxia in order to improve the outcome [2]. One such approach is carbogen (5% CO_2 balanced with O_2) breathing, which has been used either alone or in combination with nicotinamide in the treatment of tumors, especially malignant gliomas in the Accelerated Radiation, Carbogen, Nicotinamide (ARCON) studies [2]. There are, however, reports of acute toxicity, especially in the use of nicotinamide. It might be possible to achieve better radiotherapeutic outcomes even without nicotinamide, if tumor pO_2 could be measured during such treatments and radiation delivered at times of increased tumor pO_2.

Several methods have been developed to increase tumor oxygenation, such as, by using gases with high oxygen content at normobaric or hyperbaric pressures [4,5], carbogen (95% O_2 + 5% CO_2) breathing [2], administration of hypoxic-cell sensitizers [6,7], and erythropoietin to improve hemoglobin levels [8,9]. Although these methods have led to mixed results, it is generally agreed that radiotherapeutic outcome should improve, if an effective strategy is established to reduce tumor hypoxia.

Polarographic oxygen electrodes (Eppendorf Histograph) [10–12], fluorescence quenching (OxyLite) [13,14], ^{19}F-NMR spectroscopy [15–18] and BOLD MRI [19–22] and Overhauser methods

* Corresponding author. Address: EPR Center for the Study of Viable Systems, Department of Diagnostic Radiology, Dartmouth Medical School, Hanover, NH 03755, United States. Fax: +1 603 650 1717.
E-mail address: Huagang.Hou@Dartmouth.edu (H. Hou).

1090-7807/$ - see front matter Published by Elsevier Inc.
doi:10.1016/j.jmr.2011.09.043

[23] have been used to directly assess tumor pO_2 or parameters that are indirectly related to tumor pO_2. However, concerns regarding invasiveness, insufficient dynamic range of measurements, requirements for repetitive measurement, and poor spatial or temporal resolution have limited the applicability of these techniques.

Electron paramagnetic resonance (EPR) oximetry has been successfully used for repeated measurements of partial pressure of oxygen (pO_2) [24,25]. The basis of EPR oximetry is the paramagnetic nature of molecular oxygen, which therefore affects the EPR spectra of other paramagnetic species (EPR probes) in its vicinity by altering their relaxation rates. The magnitude of the effects is directly related to the amount of oxygen that is present in the environment of the paramagnetic probes (ex. lithium phthalocyanine crystals). The useful properties of LiPc for EPR oximetry are their stability and strong response of their spectra to the presence of oxygen. These are metabolically inert and are very sensitive for measuring low levels of oxygen. Once introduced in the tissue of interest, they allow repeated measurement of pO_2 at the same site for up to years after implantation. Based on extensive pre-clinical and some clinical studies [26–30], EPR oximetry with particulate paramagnetic materials has shown several advantages, especially for the repetitive and accurate measurement of localized tissue pO_2. However, these studies have also indicated the areas in which progress is needed, particularly the need for technological developments that can enable measurements in tissues at depths of greater than 10 mm. The concept of Implantable Resonators (IRs) for the measurements of tissue pO_2 was initially suggested by Swartz et al. [31]. The preliminary data suggesting the feasibility of IRs for oximetry was recently reported by Li et al. [32]. We have systematically investigated the potential application of two probe IRs for oximetry in the brain of rats. The in vitro sensitivity to oxygen and *S*/*N* ratio of two probes IRs were compared with lithium phthalocyanine (LiPc, oximetry probe) aggregates directly implanted in the phantoms. These IRs were used for repeated measurements of tissue pO_2 in the brain of normal rats and the rats with orthotopic F98 gliomas. We have also investigated the dynamic changes in the oxygenation of F98 glioma and contralateral brain (CLB) during tumor growth and hyperoxia with carbogen challenge. IRs with more than two probes could potentially be used to assess tissue pO_2 simultaneously at multiple sites by EPR oximetry.

2. Methods and materials

2.1. Tumor and animal models

All animal use procedures were in strict accordance with the NIH Guide for the Care and Use of Laboratory Animals and were approved by the Institutional Animal Care and Use Committee of Dartmouth Medical School. The experimental F98 glioma cells were purchased from ATCC (Manassas, VA) and grown in vitro using DMEM medium with 10% FBS, and 1% penicillin–streptomycin. Fischer rats (200–250 g), which are syngeneic hosts for F98 gliomas, were purchased from Charles River Laboratory (MA) and housed in the animal resource facility at Dartmouth Medical School. For injection, the cells were trypsinized and suspended in DMEM, without serum or additives.

2.2. Paramagnetic material and two probe IRs

Oxygen sensitive LiPc crystals were synthesised in our laboratory and used to construct two probe IRs. The EPR properties of LiPc have been reported earlier [24]. The resonators were assembled with thin copper wire (thickness: 0.15 mm) and has two sets of loops: a larger loop (coupling loop) on one end and transmission lines with small loops (sensor loops) on the other end. The coupling loop has a diameter of 10 mm and is used to couple inductively to the L-band (1200 MHz) EPR spectrometer. The sensor loops have a diameter of 0.2–0.3 mm, which are loaded with LiPc crystals enclosed within a gas permeable TeflonAF2400 (Sigma–Aldrich, St. Louis, MO) coating. The entire IR is then coated (10 times) with TeflonAF2400 for biocompatibility [33]. The sensor loops are implanted in the sites of interest, and the coupling loop is placed over the skull (underneath the skin) for coupling with the external loop resonator of the EPR spectrometer. (Fig. 1a and b). The total length of the transmission line is 6 mm and the distance between sensor probes is 5 mm. In general, the resonant frequency of the IRs was approximately 1183–1190 MHz in air, 1167–1185 MHz in gel and 1168–1176 MHz in vivo. The Q factors were in the range of 90–120. The diameter of the loop, the number of probes, the length of the transmissions line (depth of the probes), and the distance between them can be adjusted based on the experimental requirements.

The high density of unpaired spins combined with its narrow intrinsic line width of LiPc crystals enables the measurements of pO_2 with an area of $\sim$ 0.03–0.07 mm^2/probe. The IRs were calibrated before implantation (Fig. 1c) and the EPR spectra reflect the average pO_2 on the surface of each probe.

2.3. Multisite EPR oximetry using IRs

Male Fischer rats (200–250 g, Charles River Laboratories, Wilmington, MA) were used to inoculate intracerebral tumors in this study. For cell injection, the rats were anesthetized (2–2.5% isoflurane in 30% O_2) through a nose cone and the head were shaved, cleaned and antiseptically treated with betadine and then 70% alcohol scrubs. All surgical procedures were performed under sterile conditions. A small incision (1.5–2.0 cm) was made on the skin and two burr holes were drilled by a 23 gauge needle on the skull at predefined co-ordinates (2.5 mm left and 2.5 mm right of the midline and 3 mm posterior to the bregma). Two probe IRs were gently inserted into the brain tissue through these burr holes by using a stereotaxic frame. The depth of the sensor loops was 6 mm from the surface of the skull. For tumor inoculation, the F98 cells ($2–2.5 \times 10^5$ cells per 10 μl) were slowly injected into the brain through the left burr hole at a depth of 5.5 mm after the implantation of IRs. The holes were cleaned with alcohol prep pads, sealed with bone wax, and the skin sutured.

EPR measurements were initiated on day 7 with an L-band EPR spectrometer equipped with a microwave bridge and an external loop resonator specially designed for in vivo experiments [25,34]. The rats were placed between the poles of the EPR magnet and the external loop resonator was gently positioned on the head. The body temperature of the animals were measured by a rectal probe during EPR measurements and maintained at 37 ± 0.5 °C with a heated water blanket and warm air forced through the gap of the magnets. A set of coils capable of generating a magnetic field gradient in the direction of the magnetic field with a magnitude up to 3.0 G/cm was used to separate the EPR spectra from each probe of the IRs [35]. The peak-to-peak line widths of the EPR spectra were converted to pO_2 by using appropriate calibration of the IRs used in this study (Fig. 1c). The maximum increase in the tumor pO_2 ($pO_{2\ max}$) and the time to reach the maximum pO_2 (T_{max}) during carbogen inhalation from each implant were determined, and then averaged to obtain individual mean for each group.

The EPR settings were: incident microwave power (unsaturating): 80 mW for LiPc crystals and 0.02–0.8 mW for IRs (see below experimental design section); gradient: 56–84 mT/m; modulation frequency 24 kHz; magnetic field center 425 G; scan time 10 s, scan range 3–30 G, variable modulation amplitude not exceeding one-third of the peak-to-peak line width.

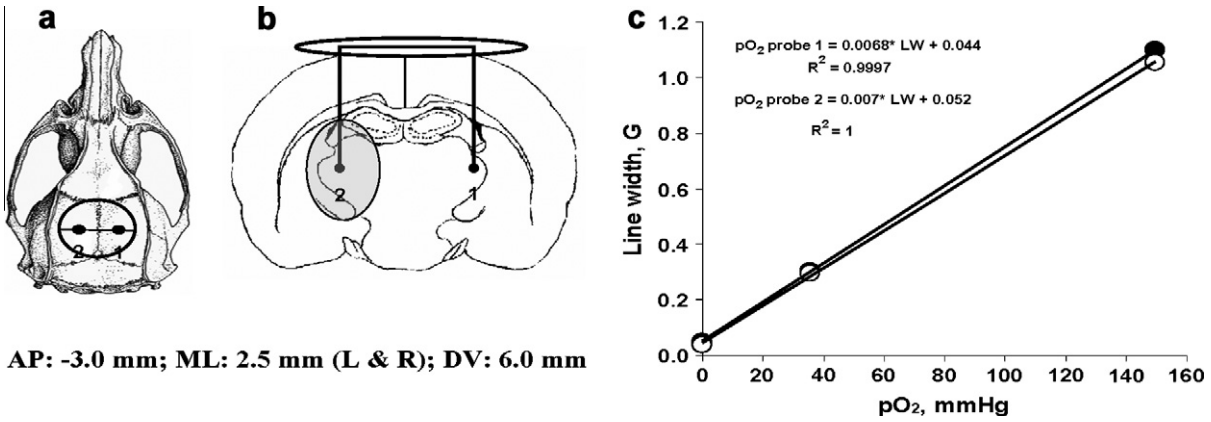

Fig. 1. (a) Axial view of rat skull with trephination positions for the IR: (b) Schematic of cross section of a rat brain showing the location of the F98 glioma (shade area) and the location of the IR in the glioma (sensor loop 2) and contralateral normal brain (sensor loop 1). AP: anterior–posterior; ML; medial–lateral; DV: dorsal–ventral. (c) The change in peak to peak line width of a 2-probe IR at different pO_2. The calibration plot shows a linear relationship between the line width and pO_2.

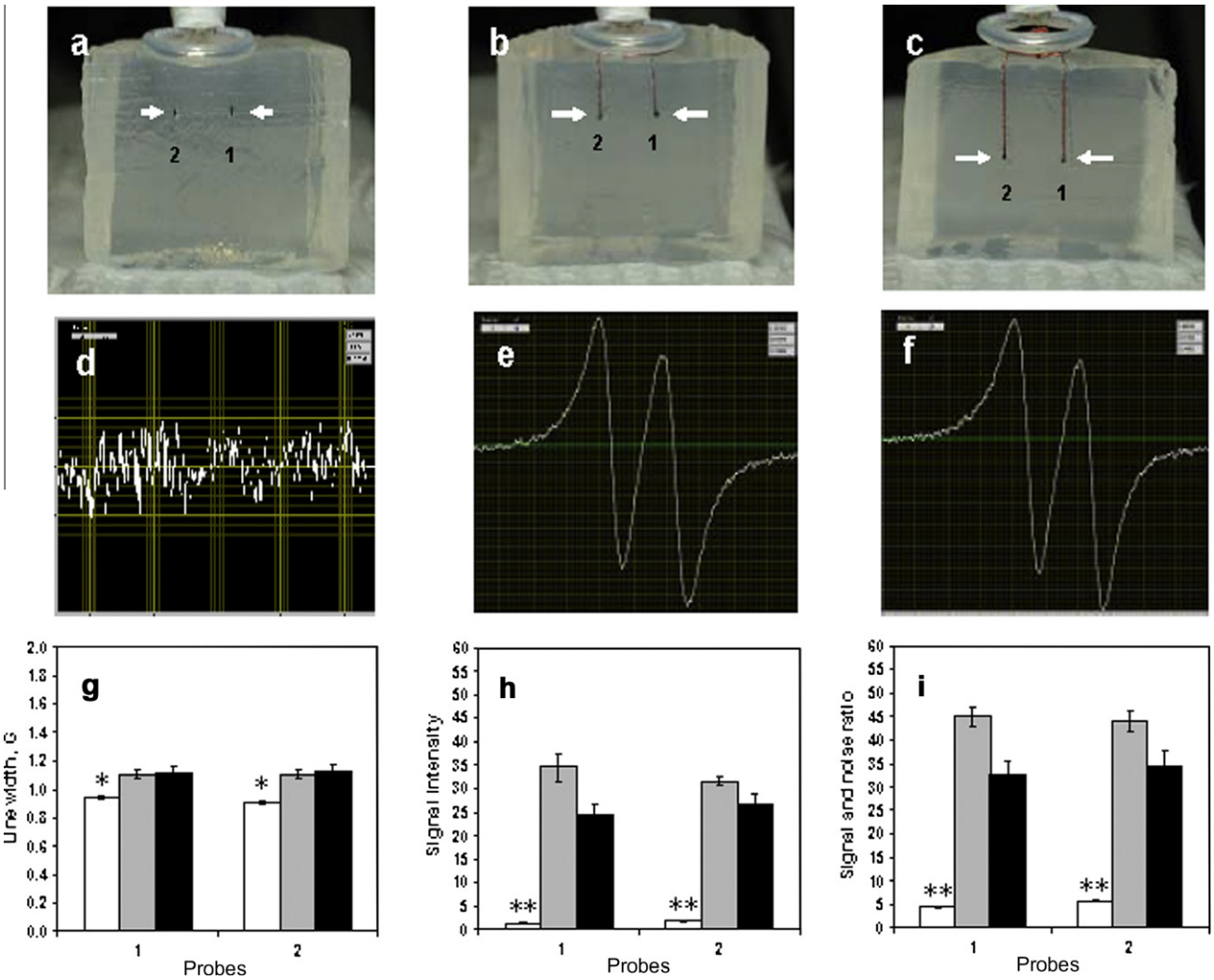

Fig. 2. Phantoms (1.5% agarose gel) used for in vitro experiments with (a) LiPc deposits, (b) IR with 6 mm transmission line and (c) IR with 11 mm transmission line. Typical EPR spectra recorded from (d) LiPc deposits, (e) IR shown in 2b, and (f) IR shown in 2c. The line widths, signal intensity and *S*/*N* ratio of the EPR signals acquired from the LiPc deposits (white column), IR with 6 mm transmission line (gray column) and IR with 11 mm transmission line (black column) are shown in 3g, 3h and 3i, respectively. $n = 3$. $^{*}p < 0.05$, $^{**}p < 0.01$, compared with IR of 6 mm and 11 mm transmission lines (unpaired *T*-test).

2.4. Magnetic resonance imaging (MRI)

The rats were imaged on day 6 after cell injection to confirm tumor growth and the location of sensor loops (probes). The MR images were acquired on a 7T horizontal magnet with a bore of 20 cm (Magnex Scientific Ltd., UK) equipped with actively shielded imaging gradients, maximum gradient strength of 77 G/cm, clear bore of 90 mm (Resonance Research Incorporated Ltd., MA), and

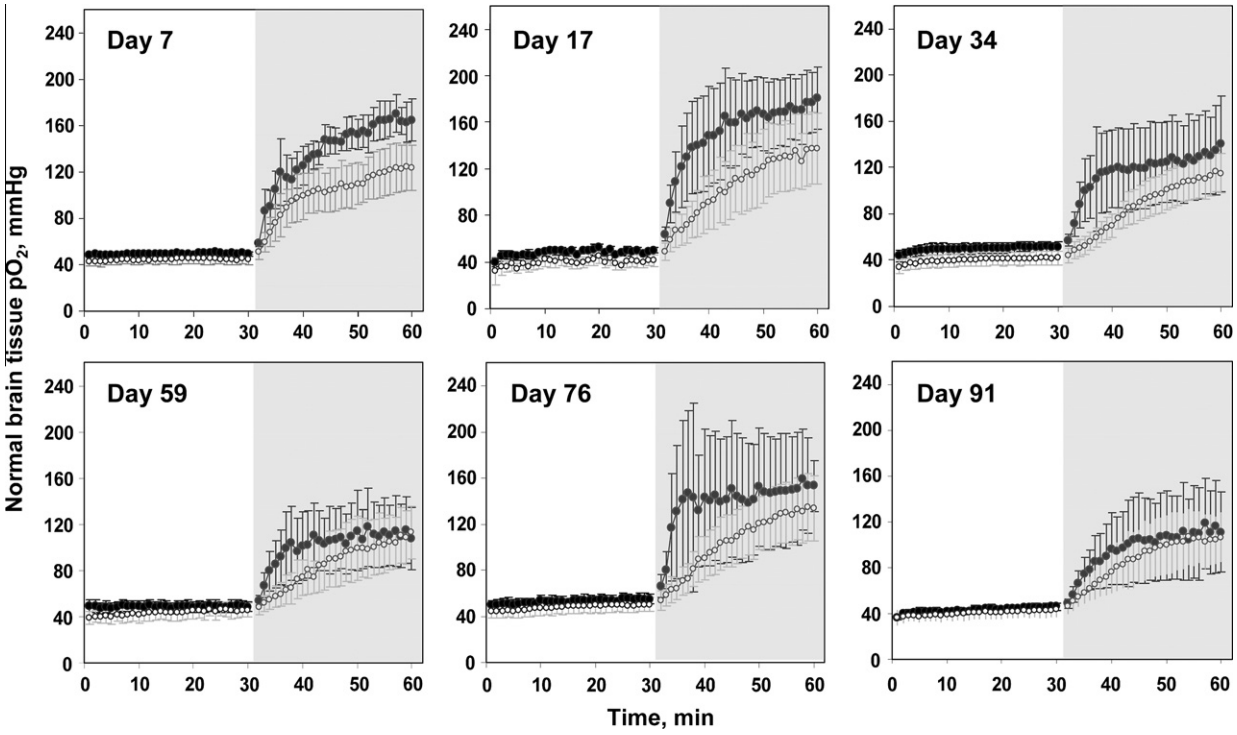

Fig. 3. Dynamics changes in the tissue pO_2 of left hemisphere (●) and right hemisphere (○) of rat brain (control group) measured by multisite EPR oximetry with 2 probe IRs during 30 min of 30% O_2 (baseline) and carbogen breathing (gray color shaded area). $N = 4$.

Table 1
Baseline pO_2 and averaged pO_2, maximum pO_2 and time to reach to maximum pO_2 during 30 min carbogen inhalation in control group.

Time (days)	$pO_{2\ base}$ (mmHg)		$pO_{2\ 30\ min\ aver.}$ (mmHg)		$pO_{2\ max}$ (mmHg)		T_{max} (min)	
	N/*L*	*N*/*R*	*N*/*L*	*N*/*R*	*N*/*L*	*N*/*R*	*N*/*L*	*N*/*R*
7	49 ± 1.3	44 ± 4.2	138 ± 12**	102 ± 27*	175 ± 18*	127 ± 35*	22 ± 5.6	28 ± 0.9
17	48 ± 2.6	40 ± 5.1	152 ± 31*	106 ± 25*	189 ± 32*	139 ± 31*	23 ± 3.6	28 ± 0.9
34	50 ± 4.4	40 ± 5.6	118 ± 32*	87 ± 13*	145 ± 41*	117 ± 18*	25 ± 5.0	29 ± 0.2
59	49 ± 4.8	44 ± 6.5	102 ± 26	86 ± 20	127 ± 32	113 ± 23*	22 ± 3.8	30 ± 0.5
76	53 ± 4.5	48 ± 6.2	142 ± 32	104 ± 21	192 ± 37	138 ± 28*	21 ± 4.7	29 ± 0.7
91	43 ± 2.8	40 ± 5.5	97 ± 31	87 ± 19	121 ± 40	111 ± 23*	23 ± 3.3	27 ± 2.0

Abbreviations: pO_2 base: baseline pO_2; $pO_{2\ 30\ min\ aver.}$: brain pO_2 averaged from 30 min carbogen inhalation; $pO_{2\ max}$: maximum pO_2; T_{max}: time to reach maximum pO_2; *N*/*L*: normal tissue/left hemisphere; *N*/*R*: normal tissue/right hemisphere. $N = 4$.
* $p < 0.05$, compared with $pO_{2\ base}$ on same day.
** $p < 0.01$, compared with $pO_{2\ base}$ on same day.

interfaced to a Varian Inova Unity console (Varian Inc., CA). Gadopentate (0.2 mmol/kg, i.p, Magnevist, Bayer Healthcare) was injected and a multi-slice spin echo sequence was used to acquire T_1-weighted images for tumor volume determination with the acquisition parameters: TR = 700 ms, TE 8 ms, 20 slices, no slice gap, slice thickness 1 mm, Field of View (FOV) = 30 mm, 128 × 128, two signal averages per phase encoding step. Tumor volumes were calculated by drawing the region of interest on the contrast enhanced tumor regions using Varian BROWSER software.

2.5. Experimental design

2.5.1. In vitro calibration of IRs

Calibrations of the IRs were performed by monitoring changes in the EPR line width when the perfused gas was switched from 0% O_2 to 5% O_2 and 21% O_2. Calibration was performed at the L-band EPR spectrometer and the spectra were fitted by a built-in MATLAB program.

2.5.2. In vitro phantom experiment

In vitro experiments were carried out in 1.5% agarose gel (phantom) to compare the sensitivity and *S*/*N* ratio of IRs with LiPc deposits. Two aggregates of LiPc (100 μg each) crystals were implanted into the gel at a distance of 5 mm and depth of 6 mm (Fig. 2a). IRs containing 50 μg of LiPc in each sensor loops were also implanted in the phantom. The distances between the probes were 5 mm and the depths (i.e. length of transmission lines) were 6 mm and 11 mm respectively (Fig. 2b and c). Three samples for each experiment were used to compare the sensitivity of IRs and LiPc deposits.

2.5.3. In vivo experiment

Ten male Fisher rats were randomly divided into two groups (control, no tumor, $N = 4$ and tumor group, $N = 6$). EPR oximetry measurements were carried out on each animal for 30 min to measure the pO_2 at the two sites and to determine its variation over time. The breathing gas was then switched to carbogen, and EPR

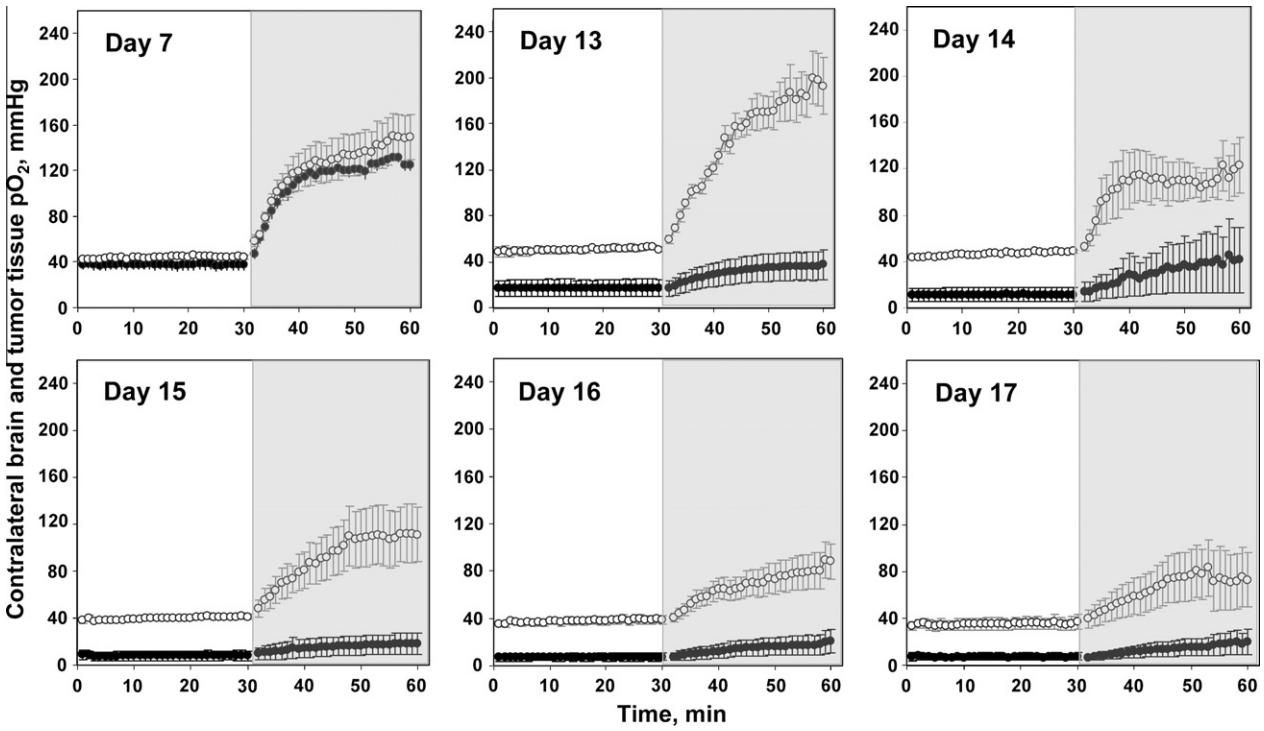

Fig. 4. Dynamic changes in the tissue pO_2 of intracranial F98 glioma (●) and contralateral brain (○) measured by multisite EPR oximetry with 2 probes IRs during 30 min of 30% O_2 (baseline) and carbogen breathing (gray color shaded area). $N = 6$.

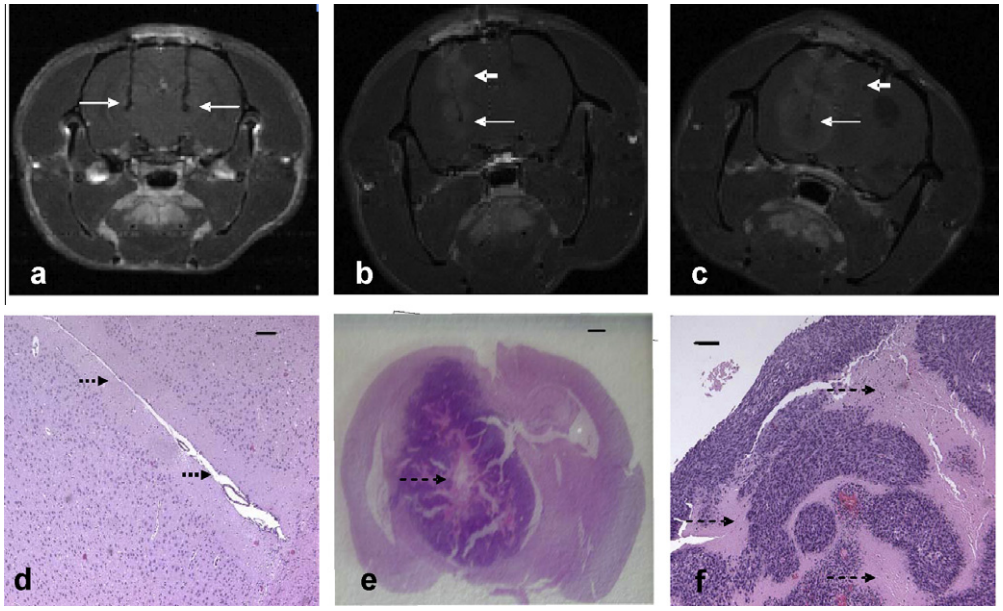

Fig. 5. MR images and H & E stained brain sections in a normal rat (a and d, control group) and rat with F98 glioma (b, c and e). (a) T1-weighted MR image on day 6 after an IR implantation; (b) T1-weighted MR image on day 12 after IR and F98 tumor cells implantation; (c) T1-weighted MR image on day 18 after IR and F98 tumor cells implantation. The arrows indicate the F98 tumor (left-hemisphere of the brain) and the positions of sensor loops. (d) H & E stained brain section shows the normal brain tissue and the track of the IRs in a control rat; (e and f) H & E stained brain section of contralateral normal brain and necrotic areas in the tumor. Magnification: 10× (d), 1× (e) and 40× (f).

measurements were continued for another 30 min. These experimental procedures were repeated on day 13–18 in the tumor group and on day 17, 34, 59, 76 and 91 in the control group.

2.6. Histological analysis

At the end of the experiments, the rats were deeply anesthetized and perfused with phosphate-buffered saline followed by 10% formalin. The IRs were removed and then the brains were sectioned and stained with H & E. The microscopic examination of the tissue was performed to confirm the position of the IRs and any histological changes in the tissue adjacent to the sensor loops and transmission lines.

2.7. Statistical analysis

Data were analyzed by student's *T* test. A paired *T* test was used to compare the pO_2 values and tumor volume within the same

Table 2
Baseline pO_2 and averaged pO_2, maximum pO_2 and time to reach to maximum pO_2 during 30 min carbogen inhalation in tumor group.

Time (days)	$pO_{2\ base}$ (mmHg)		$pO_{2\ 30\ min\ aver.}$ (mmHg)		$pO_{2\ max}$ (mmHg)		T_{max} (min)	
	T/*L*	*N*/*R*	*T*/*L*	*N*/*R*	*T*/*L*	*N*/*R*	*T*/*L*	*N*/*R*
7	38 ± 4.4	44 ± 1.6	111 ± 5**	123 ± 15**	134 ± 4**	152 ± 21**	27 ± 0.3	29 ± 0.5
13	17 ± 7.3	51 ± 3.0	31 ± ll*	148 ± 10**	38 ± 13*	213 ± 21 **	30 ± 0.3	25 ± 2.2
14	11 ± 5.9	46 ± 0.8	30 ± 19*	105 ± 18*	46 ± 11	132 ± 23*	21 ± 2.5	19 ± 3.3
15	8.0 ± 3.9	40 ± 1.7	15 ± 8	92 ± 19*	19 ± 9.1	121 ± 27*	26 ± 1.1	26 ± 1.8
16	7.2 ± 3.1	38 ± 3.0	14 ± 7	68 ± ll*	18 ± 8.6	84 ± 15*	25 ± 2.9	27 ± 1.6
17	7.0 ± 2.7	35 ± 4.9	13 ± 6	66 ± 17*	18 ± 9.0	86 ± 24*	29 ± 1.0	27 ± 1.4

Abbreviations: $pO_{2\ base}$: baseline pO_2; $pO_{2\ 30\ min\ aver.}$: brain pO_2 averaged from 30 min carbogen inhalation; $pO_{2\ max}$: maximum pO_2; T_{max}: time to reach maximum pO_2; *T*/*L*: tumor tissue/left hemisphere; *N*/*R*: normal tissue/right hemisphere. $N = 6$.
* $p<0.05$, compared with pO_2 base on same day.
** $p<0.01$, compared with pO_2 base on same day.

group. Comparisons between groups were made using a student's *T* test for unpaired samples. The tests were two-sided and a change with a *p*-value <0.05 was considered statistically significant. All data are expressed as mean ± SE; *N* is the number of animals and *n* is the number of in vitro samples.

3. Results and discussion

3.1. In vitro calibration of IRs

The line widths of the EPR spectrum acquired from each sensor loop of IRs were a linear function of pO_2, Fig 1c. Some variations in the calibration between sensor loops at higher oxygen concentrations were observed. Therefore, each sensor loop was calibrated before the implantation of the IRs, and the line width recorded from each sensor loop (probes) was converted to pO_2 using their own calibration curves.

3.2. In vitro EPR measurements in phantom (1.5% agarose gel)

The EPR spectrum obtained from the LiPc deposits and IRs are shown in Fig. 2d–f. Significant differences between the line widths of the LiPc deposits and those of IRs were noted (Fig. 2g). The intensities and *S*/*N* ratio of the EPR signals from the LiPc deposits were significantly smaller than those of IRs ($p < 0.01$, Fig. 2h and i). These results suggest that even at low power and depths of up to 11 mm, IRs provided significantly better *S*/*N* ratio than the LiPc deposits (6–10 times higher). This could potentially facilitate accurate measurements of pO_2 in deep sited tissues. The reason for the broad line width recorded from IRs as compared to that of LiPc deposits is not clear; it is perhaps due to mechanical changes in IRs and warrants further investigation.

3.3. In vivo measurement of normal brain pO_2 and the effect of hyperoxia

The baseline pO_2 in both hemispheres of the normal brain were similar on day 7, Fig. 3 and Table 1. Dynamic changes in the brain pO_2 were measured during 30% oxygen and carbogen breathing in experiments repeated on days 7, 17, 34, 59, 76 and 91. No significant differences in the mean baseline pO_2 between both hemispheres over days were observed. Carbogen inhalation resulted in significant increases in tissue pO_2 however, the maximum pO_2 and the time to reach to maximum pO_2 varied (approx. 80–220 mm Hg and 15–30 min respectively, Fig. 3 and Table 1) over days.

IRs with sensor loops at a depth of 6 mm from the surface of the skull provided strong EPR signals at low microwave power (<0.8 mW) even when a significant line broadening due to an increase in pO_2 occurred during carbogen breathing. These results indicate that IRs make it feasible to simultaneously and repeatedly assess acute changes in pO_2 at multiple sites in the brain over the entire experimental period. Spatial resolution between implants at distances of 5 mm (Figs. 2 and 5a–c) can be easily achieved by applying minimal gradient power without distortion of the EPR signals. This is a particularly useful feature of multisite EPR oximetry because the measurement from one region can be used as an internal control while other regions in the same or contralateral hemisphere could be monitored as indicators of the experimental interventions.

3.4. In vivo measurement of orthotopic F98 glioma and contralateral brain pO_2 during hyperoxia

The baseline pO_2 of F98 glioma and CLB were similar on day 7, Fig. 4 and Table 2. A gradual decline in the pO_2 of the left hemisphere (tumor) was observed, while the pO_2 of the CLB remained stable on days 13–17. A significant hypoxia was observed from day 14 with the development of F98 glioma in the left hemisphere. The maximum pO_2 and the time to reach to maximum pO_2 in CLB and the tumor during carbogen inhalation varied over days. The mean pO_2 of the CLB increased significantly during carbogen inhalation on days 7–17. On the other hand, a significant increase in the mean glioma pO_2 occurred during carbogen breathing only on day 7, day 13 and day 14 (Table 2). A significant decrease in the glioma pO_2 and response to carbogen was observed on subsequent days. These results indicate that the F98 glioma are hypoxic with a pO_2 of <10 mm Hg, consistent with our earlier findings in the studies carried out with direct LiPc implants in the F98 gliomas [36]. Similar results were obtained with the C6 gliomas, however the 9L gliomas were well oxygenated [28]. The decrease in F98 glioma pO_2 and response to carbogen over days is likely because of a decrease in tumor perfusion (compromised vasculature due to atypical angiogenesis) with the growth of glioma over days. In addition, an increase in intracranial pressure has also been reported with glioma growth [37], which could also compromise the perfusion in the gliomas.

These results confirm the feasibility of IRs for repeated measurements of orthotopic glioma pO_2 over several days. The maximum increase in tumor pO_2 and the time to reach maximum pO_2 could be potentially used to optimize chemoradiation by scheduling doses at times of increased glioma oxygenation.

3.4.1. MRI and histological analysis

The T1-weighted MR images acquired to confirm the location of the IRs in the control on day 7 and tumor groups on day 12 are shown in Fig. 5a and b, respectively. A subsequent MRI on day 17 confirmed a bulky tumor with the probes of the IR in the tumor and CLB (Fig. 5c). Histological examination showed no obvious infiltration of inflammatory cells and blood cells along the track

of the IRs (Fig. 5d) in the normal brain of rats (control group). Some accumulation of necrotic cells and blood cells were observed in the tumor (Fig. 5e and f). These results are similar to our earlier observation of minimal histological changes around LiPc implants.

4. Conclusion

In conclusion, these results confirm the feasibility of EPR oximetry using IRs in experiments involving short-term or long-term follow-up studies. The IRs provide significantly better *S*/*N* ratio as compared to direct LiPc implants, which will facilitate precise measurements of tissue pO_2 at multiple sites using EPR oximetry. This approach is currently being used to assess the tissue pO_2 at depths of 30 mm in the brain of pigs. Direct repeated measurement of glioma pO_2 is likely to play a vital role in understanding the dynamics of hypoxia during the development of gliomas. Repeated assessment of glioma pO_2 could be used to optimize therapies designed to modulate tumor hypoxia and enhance the outcome of chemoradiation by scheduling treatments at times of increased glioma pO_2.

Acknowledgments

This work was supported by NIH grants CA120919 to NK and P01EB2180 to HMS, and used the facilities of the EPR Center for the Study of Viable Systems.

References

[1] I.J. Hoogsteen, H.A. Marres, A.J. van der Kogel, J.H. Kaanders, The hypoxic tumour microenvironment, patient selection and hypoxia-modifying treatments, Clin. Oncol. (R Coll. Radiol.) 19 (2007) 385–396.
[2] J. Overgaard, Hypoxic radiosensitization: adored and ignored, J. Clin. Oncol. 25 (2007) 4066–4074.
[3] P. Vaupel, Hypoxia, aggressive tumor phenotype: implications for therapy and prognosis, Oncologist 13 (Suppl. 3) (2008) 21–26.
[4] D.M. Brizel, S. Lin, J.L. Johnson, J. Brooks, M.W. Dewhirst, C.A. Piantadosi, The mechanisms by which hyperbaric oxygen and carbogen improve tumour oxygenation, Br. J. Cancer 72 (1995) 1120–1124.
[5] M. Saunders, S. Dische, Clinical results of hypoxic cell radiosensitisation from hyperbaric oxygen to accelerated radiotherapy, carbogen and nicotinamide, Br. J. Cancer (27) (1996) S271–S278.
[6] J. Overgaard, H.S. Hansen, M. Overgaard, L. Bastholt, A. Berthelsen, L. Specht, B. Lindelov, K. Jorgensen, A randomized double-blind phase III study of nimorazole as a hypoxic radiosensitizer of primary radiotherapy in supraglottic larynx and pharynx carcinoma. Results of the Danish Head and Neck Cancer Study (DAHANCA) Protocol 5-85, Radiother. Oncol. 46 (1998) 135–146.
[7] J. Overgaard, M.R. Horsman, Modification of hypoxia-induced radioresistance in tumors by the use of oxygen and sensitizers, Semin. Radiat. Oncol. 6 (1996) 10–21.
[8] M. Henke, R. Laszig, C. Rube, U. Schafer, K.D. Haase, B. Schilcher, S. Mose, K.T. Beer, U. Burger, C. Dougherty, H. Frommhold, Erythropoietin to treat head and neck cancer patients with anaemia undergoing radiotherapy: randomised, double-blind, placebo-controlled trial, Lancet 362 (2003) 1255–1260.
[9] G. Stuben, C. Pottgen, K. Knuhmann, K. Schmidt, M. Stuschke, O. Thews, P. Vaupel, Erythropoietin restores the anemia-induced reduction in radiosensitivity of experimental human tumors in nude mice, Int. J. Radiat. Oncol., Biol., Phys. 55 (2003) 1358–1362.
[10] M.R. Horsman, A.A. Khalil, D.W. Siemann, C. Grau, S.A. Hill, E.M. Lynch, D.J. Chaplin, J. Overgaard, Relationship between radiobiological hypoxia in tumors and electrode measurements of tumor oxygenation, Int. J. Radiat. Oncol., Biol., Phys. 29 (1994) 439–442.
[11] F. Kallinowski, R. Zander, M. Hoeckel, P. Vaupel, Tumor tissue oxygenation as evaluated by computerized-pOz_2-histography, Int. J. Radiat. Oncol., Biol., Phys. 19 (1990) 953–961.
[12] J.A. O'Hara, N. Khan, H. Hou, C.M. Wilmo, E. Demidenko, J.F. Dunn, H.M. Swartz, Comparison of EPR oximetry and Eppendorf polarographic electrode assessments of rat brain PtO_2, Physiol. Meas. 25 (2004) 1413–1423.
[13] J.R. Griffiths, S.P. Robinson, The OxyLite: a fibre-optic oxygen sensor, Br. J. Radiol. 72 (1999) 627–630.
[14] J.A. O'Hara, H. Hou, E. Demidenko, R.J. Springett, N. Khan, H.M. Swartz, Simultaneous measurement of rat brain cortex PtO_2 using EPR oximetry and a fluorescence fiber-optic sensor during normoxia and hyperoxia, Physiol. Meas. 26 (2005) 203–213.
[15] R.P. Mason, P.P. Antich, E.E. Babcock, A. Constantinescu, P. Peschke, E.W. Hahn, Non-invasive determination of tumor oxygen tension and local variation with growth, Int. J. Radiat. Oncol., Biol., Phys. 29 (1994) 95–103.
[16] J.A. Raleigh, A.J. Franko, D.A. Kelly, L.A. Trimble, P.S. Allen, Development of an in vivo 19F magnetic resonance method for measuring oxygen deficiency in tumors, Magnet. Reson. Med. 22 (1991) 451–466.
[17] B.F. Jordan, G.O. Cron, B. Gallez, Rapid monitoring of oxygenation by 19F magnetic resonance imaging: simultaneous comparison with fluorescence quenching, Magnet. Reson. Med. 61 (2009) 634–638.
[18] J. Magat, B.F. Jordan, G.O. Cron, B. Gallez, Noninvasive mapping of spontaneous fluctuations in tumor oxygenation using 19F MRI, Med. Phys. 37 (2010) 5434–5441.
[19] C. Baudelet, B. Gallez, How does blood oxygen level-dependent (BOLD) contrast correlate with oxygen partial pressure (pO_2) inside tumors?, Magnet Reson. Med. 48 (2002) 980–986.
[20] J.F. Dunn, J.A. O'Hara, Y. Zaim-Wadghiri, H. Lei, M.E. Meyerand, O.Y. Grinberg, H. Hou, P.J. Hoopes, E. Demidenko, H.M. Swartz, Changes in oxygenation of intracranial tumors with carbogen: a BOLD MRI and EPR oximetry study, J. Magn. Reson. Imag. 16 (2002) 511–521.
[21] L.D. McPhail, S.P. Robinson, Intrinsic susceptibility MR imaging of chemically induced rat mammary tumors: relationship to histologic assessment of hypoxia and fibrosis, Radiology 254 (2010) 110–118.
[22] L.M. Rodrigues, F.A. Howe, J.R. Griffiths, S.P. Robinson, Tumor $R2^*$ is a prognostic indicator of acute radiotherapeutic response in rodent tumors, J. Magn. Reson. Imag. 19 (2004) 482–488.
[23] M.C. Krishna, S. English, K. Yamada, J. Yoo, R. Murugesan, N. Devasahayam, J.A. Cook, K. Golman, J.H. Ardenkjaer-Larsen, S. Subramanian, J.B. Mitchell, Overhauser enhanced magnetic resonance imaging for tumor oximetry: coregistration of tumor anatomy and tissue oxygen concentration, Proc. Natl. Acad. Sci. USA 99 (2002) 2216–2221.
[24] K.J. Liu, P. Gast, M. Moussavi, S.W. Norby, N. Vahidi, T. Walczak, M. Wu, H.M. Swartz, Lithium phthalocyanine: a probe for electron paramagnetic resonance oximetry in viable biological systems, Proc. Natl. Acad. Sci. USA 90 (1993) 5438–5442.
[25] H.M. Swartz, R.B. Clarkson, The measurement of oxygen in vivo using EPR techniques, Phys. Med. Biol. 43 (1998) 1957–1975.
[26] H. Hou, N. Khan, O.Y. Grinberg, H. Yu, S.A. Grinberg, S. Lu, E. Demidenko, R.P. Steffen, H.M. Swartz, The effects of Efaproxyn (efaproxiral) on subcutaneous RIF-1 tumor oxygenation and enhancement of radiotherapy-mediated inhibition of tumor growth in mice, Radiat.Res. 168 (2007) 218–225.
[27] H. Hou, J.P. Lariviere, E. Demidenko, D. Gladstone, H. Swartz, N. Khan, Repeated tumor pO(2) measurements by multi-site EPR oximetry as a prognostic marker for enhanced therapeutic efficacy of fractionated radiotherapy, Radiother. Oncol. 91 (2009) 126–131.
[28] N. Khan, H. Li, H. Hou, J.P. Lariviere, D.J. Gladstone, E. Demidenko, H.M. Swartz, Tissue pO(2) of orthotopic 9L and C6 gliomas and tumor-specific response to radiotherapy and hyperoxygenation, Int. J. Radiat. Oncol., Biol., Phys. 73 (2009) 878–885.
[29] N. Khan, B.B. Williams, H. Hou, H. Li, H.M. Swartz, Repetitive tissue pO_2 measurements by electron paramagnetic resonance oximetry: current status and future potential for experimental and clinical studies, Antioxid. Redox Signaling 9 (2007) 1169–1182.
[30] H.M. Swartz, N. Khan, J. Buckey, R. Comi, L. Gould, O. Grinberg, A. Hartford, H. Hopf, H. Hou, E. Hug, A. Iwasaki, P. Lesniewski, I. Salikhov, T. Walczak, Clinical applications of EPR: overview and perspectives, NMR in Biomed. 17 (2004) 335–351.
[31] H.M. Swartz, T. Walczak, Developing in vivo EPR oximetry for clinical use, Adv. Exp. Med. Biol. 454 (1998) 243–252.
[32] H. Li, H. Hou, A. Sucheta, B.B. Williams, J.P. Lariviere, M.N. Khan, P.N. Lesniewski, B. Gallez, H.M. Swartz, Implantable resonators – a technique for repeated measurement of oxygen at multiple deep sites with in vivo EPR, Adv. Exp. Med. Biol. 662 (2010) 265–272.
[33] M. Dinguizli, S. Jeumont, N. Beghein, J. He, T. Walczak, P.N. Lesniewski, H. Hou, O.Y. Grinberg, A. Sucheta, H.M. Swartz, B. Gallez, Development and evaluation of biocompatible films of polytetrafluoroethylene polymers holding lithium phthalocyanine crystals for their use in EPR oximetry, Biosens. Bioelectron. 21 (2006) 1015–1022.
[34] H. Hirata, T. Walczak, H.M. Swartz, Electronically tunable surface-coil-type resonator for L-band EPR spectroscopy, J. Magn. Reson. 142 (2000) 159–167.
[35] A.I. Smirnov, S.W. Norby, R.B. Clarkson, T. Walczak, H.M. Swartz, Simultaneous multi-site EPR spectroscopy in vivo, Magnet. Reson. Med. 30 (1993) 213–220.
[36] N. Khan, S. Mupparaju, S.K. Hekmatyar, H. Hou, J.P. Lariviere, E. Demidenko, D.J. Gladstone, R.A. Kauppinen, H.M. Swartz, Effect of hyperoxygenation on tissue pO_2 and its effect on radiotherapeutic efficacy of orthotopic F98 gliomas, Int. J. Radiat. Oncol., Biol., Phys. 78 (2010) 1193–1200.
[37] T. Beppu, K. Kamada, Y. Yoshida, H. Arai, K. Ogasawara, A. Ogawa, Change of oxygen pressure in glioblastoma tissue under various conditions, J. Neuro-oncol. 58 (2002) 47–52.